



Published in final edited form as:

*Int J Cancer*. 2006 November 1; 119(9): 2236–2241.

## MicroCT for high-resolution imaging of ectopic pheochromocytoma tumors in the liver of nude mice

Shoichiro Ohta<sup>1</sup>, Edwin W. Lai<sup>1</sup>, John C. Morris<sup>2</sup>, Douglas A. Bakan<sup>3</sup>, Brenda Klaunberg<sup>4</sup>, Susannah Cleary<sup>5,6</sup>, James F. Powers<sup>7</sup>, Arthur S. Tischler<sup>7</sup>, Mones Abu-Asab<sup>8</sup>, Daniel Schimel<sup>4,9</sup>, and Karel Pacak<sup>1,\*</sup>

<sup>1</sup>Reproductive Biology and Medicine Branch, National Institute of Child Health and Human Development, Bethesda, MD

<sup>2</sup>Metabolism Branch, Center for Cancer Research, National Cancer Institute, Bethesda, MD

<sup>3</sup>Alerion Biomedical Inc., San Diego, CA

<sup>4</sup>Mouse Imaging Facility, National Institute of Neurological Disorders and Stroke, Bethesda, MD

<sup>5</sup>Clinical Neurocardiology Section, National Institute of Neurological Disorders and Stroke, Bethesda, MD

<sup>6</sup>Molecular Neurobiology, Laboratory Division of Health Sciences, Murdoch University, Perth, Australia

<sup>7</sup>Department of Pathology, Tufts New England Medical Center, Tufts University School of Medicine, Boston, MA

<sup>8</sup>Pathology Branch, Center for Cancer Research, National Cancer Institute, Bethesda, MD

<sup>9</sup>Charles River Laboratories, Inc., Germantown, MD

### Abstract

Successful outcomes for patients with cancer often depend on the early detection of tumor and the prompt initiation of active therapy. Despite major advances in the treatment of many cancers, early-stage lesions often go undetected due to the suboptimal resolution of current anatomical and functional imaging modalities. This limitation also applies to preclinical animal tumor models that are crucial for the evaluation and development of new therapeutic approaches to cancer. We report a new mouse model of metastatic pheochromocytoma, generated using tail vein injection of the mouse pheochromocytoma cell (MPC) line that reproducibly generated multiple liver tumors in the animals. Furthermore, we show that *in vivo* microCT imaging enhanced using a hepatobiliary-specific contrast agent, glyceryl-2-oleyl-1,3-di-7-(3-amino-2,4,6-triodophenyl)-heptanoate (DHO), detected tumors as small as 0.35 mm as early as 4 weeks after the injection of the tumor cells. This model may be useful for *in vivo* studies of tumor biology and for development of new strategies to treat metastatic pheochromocytoma.

### Keywords

microCT; mouse model; pheochromocytoma; liver tumor

---

Pheochromocytomas are rare neuroendocrine tumors that arise from adrenal chromaffin cells. Secretion of catecholamines by these tumors may result in clinical hypertension. They account for 0.05-0.1% of all patients with sustained hypertension.<sup>1</sup> Up to 36% of sporadic

---

\*Correspondence to: Unit on Clinical Neuroendocrinology, RBMB, NICHD, NIH, Building 10, CRC, Room 1-3140, 10 Center Drive MSC-1109, Bethesda, MD 20892-1109 USA. Fax: +1-301-402-4712. E-mail: karel@mail.nih.gov

pheochromocytomas will undergo malignant transformation with frequent spread to the liver.<sup>2,3</sup> Patients diagnosed with malignant pheochromocytoma have an overall 5-year survival of about 50%.<sup>4</sup> Once metastasized, however, there is no curative therapy for this disease.<sup>5</sup> The ability to develop effective treatments requires the availability of relevant preclinical models to test novel agents and approaches for their activity against tumor. The use of suitable laboratory animal models enhances the speed with which pheochromocytoma can be studied and new treatments evaluated. This is particularly true in the case of uncommon malignancies where comprehensive clinical trials are often lacking. The establishment of relevant animal models of metastatic pheochromocytoma is of critical importance to meet this need.

MicroCT imaging has been instrumental in the study of numerous cancers and is a promising tool for detecting and monitoring tumor growth, as well as for assessing the efficacy of anticancer therapies in small animal models.<sup>6,7</sup> In the last 5 years, commercial MicroCT scanners have been introduced for general laboratory use. These scanners offer an excellent spatial resolution of less than 50  $\mu\text{m}$  and allow for animals to undergo serial scans.<sup>6,7</sup> Because of these features, microCT imaging has the potential to allow for detailed anatomical imaging of small animals and can also serve as a powerful means to monitor tumor growth and response in small animal tumor models. Despite exceptional resolution, poor soft tissue contrast makes tumor detection with microCT difficult without the use of contrast-enhancing agents. Resolution and imaging speeds vary and are limited by the capabilities of the model of microCT scanner.<sup>8,9</sup> Unfortunately, for the highest resolution scans, comparatively long acquisition times (typically 10-20 min) are required; thus, the rapid renal clearance of conventional water-soluble imaging agents precludes their use in this setting.<sup>6</sup> There is a need, therefore, for suitably designed, longer-lasting contrast agents that exhibit low toxicity, to facilitate the detection of focal lesions in soft tissue. In the case of hepatic tumors, long-lasting hepatobiliary contrast agents may allow small liver lesions to be distinguished from normal liver tissue.

A recently developed hepatobiliary contrast agent, 20% oil-in-water emulsion of glyceryl-2-oleyl-1,3-di-7-(3-amino-2,4,6-triiodophenyl)-heptanoate (DHOG), was shown to provide superior long-lasting visualization in microCT imaging studies, especially of the liver.<sup>10-14</sup>

In the current study, we sought to establish an animal model of pheochromocytoma with ectopic liver lesions and evaluate DHOG contrast-enhanced microCT for its sensitivity in detection of liver metastases.

## Material and methods

### Cell lines

Mouse pheochromocytoma cells (MPC, 4/30 PRR)<sup>15</sup> were maintained in RPMI 1640 containing 10% heat-inactivated horse serum, 5% fetal bovine serum and antibiotics. MPC cells were grown in tissue culture dishes without collagen.

### Animals and tumor model

About 6- to 10-week-old female athymic nude mice (NCr-nu) were purchased from Taconic (Germantown, NY) and treated in accordance with institutional guidelines. To generate tumors *in vivo*, un-anesthetized mice underwent tail vein injection with  $10 \times 10^6$  MPC cells suspended in a volume of 100  $\mu\text{L}$  PBS (Sigma Chemicals Co., St. Louis, MO) using 1 mL tuberculin syringes (Becton Dickinson, Franklin Lakes, NJ) with 30-gauge hypodermic needles.<sup>16</sup> Mice were observed 3 times weekly for evidence of tumor growth or adverse effects (*e.g.*, distress, ascites, bleeding, paralysis or excessive weight loss). In preliminary studies we used a different mouse strain (NMRI) to establish this model; however, nude mice (NCr-nu) were determined to be the optimal model as they reproducibly generated hepatic lesions. This might suggest that

antitumor immune response plays an important role in controlling pheochromocytoma. This work, however, was beyond the scope of the present study. The mice were treated in accordance with the procedures approved and recommended by National Institute of Child Health and Human Development, Animal Care and Use Committee, and NIH Animal Research Advisory Committee document entitled *Endpoints in Animal Study Proposal*.

### Contrast agent administration

Mice received a tail vein injection of DHOG (Fenestra™ LC, Alerion Biomedical, San Diego, CA) at a dose of 0.013 mL/g of body weight 3 hr prior to scanning. The timing of image acquisition was selected on the basis of previous studies defining the pharmacokinetic and dose-response profiles of the agent.<sup>10,17</sup> Anesthesia was induced with 5% isoflurane and maintained at 1-2% for the duration of the scan with mice breathing spontaneously *via* mask. All mice recovered from anesthesia within 5 min after scan completion. MicroCT was performed prior to tumor cell injection and at 3, 4 and 5 weeks after injection (Fig. 1). The animals tolerated the repeated administration of DHOG without any visible signs of toxicity. To reduce additional radiation exposure to mice, experimental procedures and number of mice used, we minimized scans to prior to injection and weeks 3, 4 and 5 after injection.

### MicroCT imaging

Images were obtained on an ImTek MicroCT scanner (MicoCAT-II, ImTek, Knoxville, TN). The X-ray voltage was set at 70 kVp; an anode current 500  $\mu$ A and a shutter speed of 500 msec. Scans were completed over 360° of rotation with 900 projections to reduce signal noise. Scans were performed using a cone beam filtered back projection algorithms. To include the entire liver, a transaxial field of view was set at 3.50 cm and the axial field of view was 3.25 cm with a spatial resolution of 60  $\mu$ m. Gray-scale value of the liver before contrast application ranged between 40 and 60 Hounsfield units (HU) and after contrast enhancement between 0 and 263 HU. Laser alignment marks provided for precise positioning. Mice were not fasting before the scan; therefore, food in stomach may have accounted for some shifts in liver position. Respiratory gating was used to reduce movement artifact with images being captured at peak expiration. Although peak inspiration is usually ideal for abdominal images, the speed of the shutter was too slow to capture the images at peak inspiration. The slower shutter speed was optimal for soft tissue resolution. The total scan time for each scan was 35 min.

### Image analysis

Image data were acquired and reconstructed using ImTek software (MicroCAT Data Acquisition v 3.0; ImTek). The microCT image data from each mouse were analyzed by using commercially available visualization software (Amira, Version 3.1, TGS, San Diego, CA), which displayed the data as 2D axial, sagittal and coronal cross-sectional images. The version of Amira used is a windows based graphical interface for image reconstruction data visualization, and quantitative analysis. The data visualization package is based on IDL and includes a variety of tools, including 3D volume rendering, arbitrary 2D slice visualization and pseudo-color. Images were evaluated using Amira software and allowed for visualization and 3D rendering of the contrast-enhanced liver (Fig. 2). The voxel size was 60  $\mu$ m.

### Necropsy

Five weeks after injection of the MPC cells, mice were euthanized with carbon dioxide in compliance with institutional requirements. The abdominal cavity was opened, inspected and the abdominal organs removed “en bloc.” After dissection, the liver, GI tract and other visceral organs were examined for tumors. The livers with tumor were dissected and divided, with 1 portion fixed in formalin and embedded in paraffin for H&E and immunohistochemistry, 1

part processed for electron microscopy and the third portion of liver with tumor was reserved for catecholamine measurements.

### Immunohistochemistry and confocal microscopy

Immunohistochemical staining using antibodies directed against tyrosine hydroxylase was conducted to confirm the presence of catecholamine producing cells, according to previously published method.<sup>18</sup> The primary antibody consisted of a mouse monoclonal antityrosine hydroxylase (1:250; Immunostar, Hudson, WI), and the secondary antibody consisted of a donkey anti-mouse fluorescein isothiocyanate (FITC; 1:500; Jackson ImmunoResearch Laboratories, West Grove, PA). Liver sections not treated with primary antibody were processed concurrently as negative controls. Sections were examined using a Zeiss LSM PASCAL 5 confocal microscope equipped with Ar/Kr 488-514 filter used to excite Cy-3 and FITC. (Zeiss, Thornwood, NY). Multipass emissions were collected through the following: FITC, bandpass 505-530 using a 25× NeoFluor objective lens. Pinhole detector gain and laser power were adjusted accordingly to acquire ~5-µm-thick sections with few saturated pixels. Images were acquired with LSM 5 Image Browser software (Zeiss) and assembled using PowerPoint (Microsoft, Redmond, WA). While overall contrast was adjusted for quality, no other modifications were made.

### Electron microscopy and catecholamine measurements

To visualize catecholamine storage vesicles and other ultrastructural details, electron microscopy was performed. Specimens were double-fixed in PBS-buffered glutaraldehyde (2.5%) and osmium tetroxide (0.5%), dehydrated and embedded in Spurr's epoxy resin. Ultrathin sections (90 nm) were made and double-stained with uranyl acetate and lead citrate, and viewed in a Philips CM10 transmission electron microscope (FEI, Hillsboro, OR). Tumor catecholamine levels were measured using HPLC.<sup>19</sup>

## Results

Tail vein injection of  $10 \times 10^6$  MPC cells in athymic nude mice reproducibly generated multiple liver tumors in all animals ( $N = 8$ ) that could be visualized early in their development utilizing DHOG contrast-enhanced microCT. Localized hepatic lesions as small as 0.35 mm could be readily detected as early as 4 weeks after the injection of tumor cells (Fig. 1). Moreover, using the hepatobiliary contrast enhancement agent, tumors could be exceptionally well delineated from normal liver tissue. No distinction between tumor and liver tissue could be made in the mice scanned at week 5 without DHOG contrast showed (Fig. 3). These tumors were confirmed by necropsy at week 5. Ectopic liver tumors were characterized as pheochromocytoma by histology, immunohistological staining for tyrosine hydroxylase, ultrastructural detection of catecholamine storage vesicles and increased tumor catecholamine levels (Figs. 4 and 5).

## Discussion

This study describes the establishment of a mouse liver model of pheochromocytoma using murine MPC cells. In this model, mice developed lesions in the liver that showed classic histological and ultrastructural appearance of pheochromocytoma as well as expression of tyrosine hydroxylase. In addition, we used this model to evaluate the sensitivity of DHOG hepatobiliary contrast-enhanced microCT imaging in detecting and monitoring the growth of the liver metastases. Our results show that multiple liver tumors as small as 0.35 mm were established and could be visualized as early as 4 weeks post-injection.

Murine and other small models have come into widespread use in the preclinical testing of anticancer agents. Historically, most small animal tumor models have involved the

subcutaneous implantation of tumor cells. More relevant models involve either implanting tumors in an organ of interest, or the use of transgenic animals that give rise to tumors.<sup>21</sup> Tail vein injection models of metastatic cancer have recently been established in number of cancers, including neuroblastoma, melanoma and pancreatic cancer.<sup>16,22-24</sup> In a nude rat catecholamine secreting neuroblastoma model, tumor cells injected in the tail vein resulted in micrometastatic spread to the liver and femur.<sup>16</sup> Studies in this model demonstrated the ability of naturally occurring cytotoxic antineuroblastoma human IgM antibodies to eradicate the neuroblastoma cells.

The present study suggests that DHOG hepatobiliary contrast-enhanced microCT imaging is highly sensitive for detection and monitoring the growth of these liver lesions. Although microCT imaging has the potential for high spatial resolution, without the aid of contrast enhancement, imaging of tumors in the liver is nearly impossible due to inherently poor soft tissue contrast density. At best, necrotic areas might be detectable in the core of a liver lesion, but accurate assessment of the extent of the tumor involvement remains challenging. MicroCT scanning using targeted contrast agents such as DHOG are an effective means to detect small liver tumors in live animals.

One potential difficulty of our method involves the ability to distinguish small blood vessels imaged in cross section from tumor. Scanning at later time points after administration of DHOG (beyond 2-3 hr) may be required to assure optimal enhancement. At these time points, the contrast agent has been cleared from the vasculature. Because DHOG does not enhance tumor tissue, the intensity of a small lesion may be similar to that of blood vessels. In 2D images, small circular hypointense areas may represent either a blood vessel in cross section or a focal lesion. A solution to this problem is to administer a second dose of contrast agent to opacify the vessels to distinguish them from tumor. Another potential solution is to use the 3D data sets to track the shapes of the lesion. Whereas tumors tend to have reasonably well defined, nearly spherical boundaries, blood vessels take a tubular appearance in the image datasets. Quickly scrolling through the images distinguishes between vessels and tumor in virtually all instances. In this study, we evaluated the 3D data sets to make this distinction.

An essential component of cancer research is accurate determination of the extent of tumors in animal models. Many small animal tumor models have historically involved subcutaneous implantation of tumor fragments or tumor cells. More relevant murine models involve either the direct inoculation of tumor cells into the organ of interest mimicking the clinical situation, or use of spontaneously arising tumors in transgenic animal models.<sup>25</sup> These models have come into wider use in the preclinical testing of anticancer agents. The difficulty in using many of these animal models is the limited ability to accurately evaluate for early development and growth of intra-abdominal or visceral tumors without having to prematurely terminate the experiment and sacrifice the study animal.

This new ectopic pheochromocytoma mouse model utilizes MPC cells. The MPC cell line was isolated from heterozygous Nf1 knockout mice.<sup>25</sup> MPC cells are functionally similar to clinical human pheochromocytomas, producing both epinephrine and norepinephrine.<sup>25</sup> Of the mice undergoing tail vein injection of MPC cells, all 8 developed hepatic metastases by 4-weeks post-injection. The liver lesions showed the classic histological appearance of pheochromocytoma. Secretory vesicles in electronic microscopy and tyrosine hydroxylase in immunohistochemistry.<sup>26,27</sup> Furthermore, the tumors also expressed high levels of norepinephrine. This preclinical MPC model is relevant for the study of human pheochromocytoma. Despite attempts to establish human pheochromocytoma cell lines and several initially promising reports, human pheochromocytoma cell lines that retain a significant degree of catecholaminergic differentiation have yet to become available. The MPC model is an appropriate model because of its similarity to the human disease.<sup>21</sup> Results from ongoing

studies in our animal model may soon be extrapolated to patients with advanced malignant pheochromocytoma.

Drawbacks of our model include the large number of metastatic lesions that develop in the liver compared to other organ sites. In our model, metastatic lesions were only occasionally observed in other organs such as the lung and kidney. Also the use of the nude mouse background limits studies using immunological approaches to treatment of pheochromocytoma. We are optimistic that this model represents an accurate clinical translational picture. The majority of patients succumbing to malignant pheochromocytoma develop metastatic liver lesions. Indeed, patients with metastatic pheochromocytoma to other sites such as bone metastases exhibit far superior survivals.<sup>3,28</sup> Our current efforts are focused on the early detection, monitoring, molecular biology, genetics and treatment of metastatic pheochromocytoma. At present, there is no curative therapy, and radiation or chemotherapy are of modest benefit.<sup>4,29,30</sup> However, an intensive search for new therapies is ongoing. The introduction of new and promising drugs cannot happen without preclinical testing in relevant animal models. Thus, our model of metastatic hepatic pheochromocytoma might serve as such model. MicroCT imaging coupled with DHOGE hepatobiliary contrast enhancement is promising as a technique to longitudinally monitor the response to experimental therapy. Finally, assaying secretion of catecholamines and their metabolites by tumors can be useful for detecting biochemical changes and therefore reflect clinical responses to experimental treatment.

In future studies with our model, we expect to combine the high-resolution imaging afforded by DHOGE contrast-enhanced microCT to pathologically and physiologically study metastatic liver lesions and to accurately correlate changes in tumor volume with disease progression and the effects of our therapy. Additionally, the effects of cumulative radiation exposure of repeated microCT scanning on tumor development and therapeutic response need to be evaluated.<sup>8,9</sup>

#### Acknowledgements

This study was supported in part by NIH grant (AS Tischler). The authors are grateful to Dr. Graeme Eisenhofer and Ms. Shiromi Perera for their thoughtful comments, and Ms. Priya Kaji for her assistance in the preparation of this article.

Grant sponsor: NIH; Grant number: R01 NS 37685.

#### References

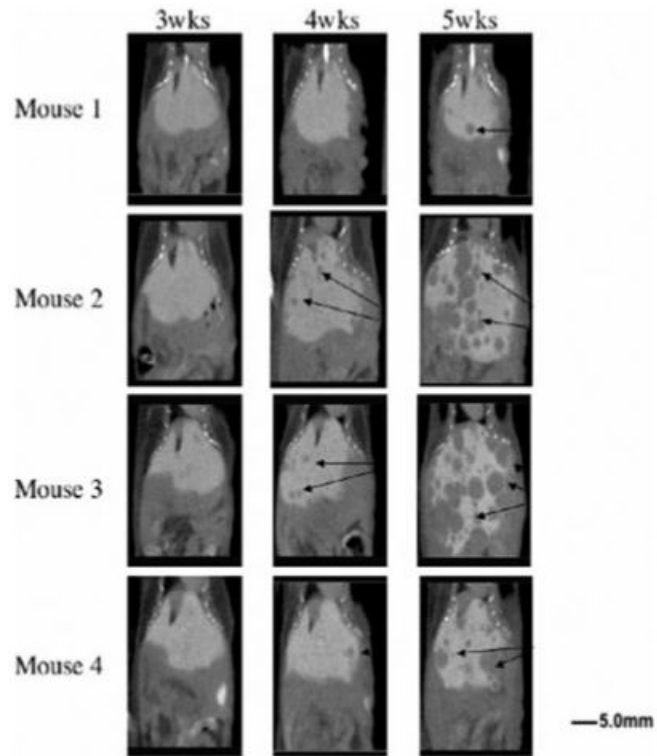
1. Pacak, K.; Chrousos, GP.; Koch, CA.; Lenders, JWM.; Eisenhofer, G. Pheochromocytoma: Progress in Diagnosis, Therapy, and Genetics. In: Margioris, AN.; Chrousos, GP., editors. Adrenal disorders. Humana Press; New Jersey: 2001. p. 379-413.
2. Goldstein RE, O'Neill JA Jr, Holcomb GW III, Morgan WM III, Neblett WW III, Oates JA, Brown N, Nadeau J, Smith B, Page DL, Abumrad NN, Scott HW Jr. Clinical experience over 48 years with pheochromocytoma. *Ann Surg* 1999;229:755-64. [PubMed: 10363888]
3. Kebebew E, Duh QY. Benign and malignant pheochromocytoma: diagnosis, treatment, and follow-up. *Surg Oncol Clin N Am* 1998;7:765-89. [PubMed: 9735133]
4. John H, Ziegler WH, Hauri D, Jaeger P. Pheochromocytomas: can malignant potential be predicted? *Urology* 1999;53:679-83. [PubMed: 10197840]
5. Pacak K, Linehan WM, Eisenhofer G, Walther MM, Goldstein DS. Recent advances in genetics, diagnosis, localization, and treatment of pheochromocytoma. *Ann Intern Med* 2001;134:315-29. [PubMed: 11182843]
6. Marx J. Imaging. Animal models: live and in color. *Science* 2003;302:1880-2. [PubMed: 14671264]
7. Kurth AA, Muller R. The effect of an osteolytic tumor on the three-dimensional trabecular bone morphology in an animal model. *Skeletal Radiol* 2001;30:94-8. [PubMed: 11310206]



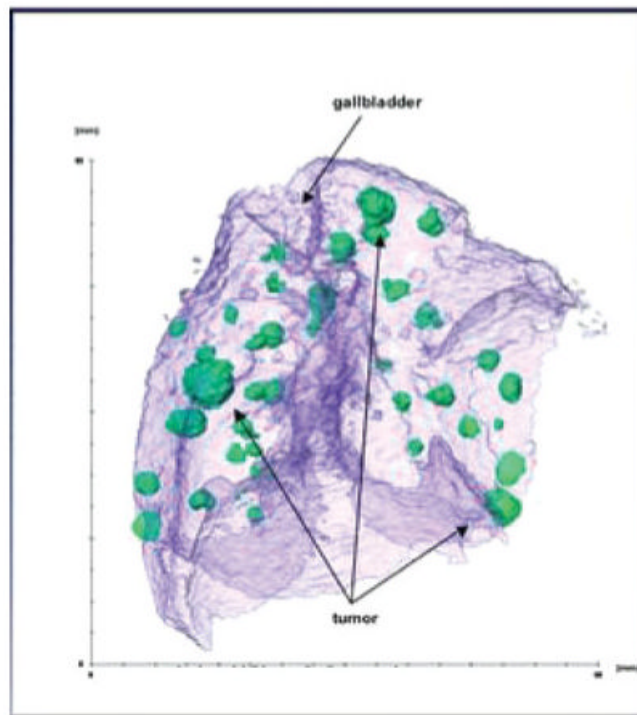
8. Mitchel RE, Jackson JS, Morrison DP, Carlisle SM. Low doses of radiation increase the latency of spontaneous lymphomas and spinal osteosarcomas in cancer-prone, radiation-sensitive Trp53 heterozygous mice. *Radiat Res* 2003;159:320–7. [PubMed: 12600234]
9. Boone JM, Velazquez O, Cherry S. Small-animal X-ray dose from micro-CT. *Mol Imaging* 2004;3:149–58. [PubMed: 15530250]
10. Bakan DA, Weichert JP, Longino MA, Counsell RE. Polyiodinated triglyceride lipid emulsions for use as hepatoselective contrast agents in CT: effects of physicochemical properties on biodistribution and imaging profiles. *Invest Radiol* 2000;35:158–69. [PubMed: 10719825]
11. Bakan DA, Doerr-Stevens JK, Weichert JP, Longino MA, Lee FT Jr, Counsell RE. Imaging efficacy of a hepatocyte-selective polyiodinated triglyceride for contrast-enhanced computed tomography. *Am J Ther* 2001;8:359–65. [PubMed: 11550077]
12. Doerr-Stevens JK, Bakan DA, Lee FT Jr, Chosy SG, Markhardt BK, Bonneville AK, Burrascano C, Delaney C, Longino MA, Greener Y, Weichert JP. Imaging efficacy of a hepatocyte-selective polyiodinated triglyceride (DHOG-LE) for contrast-enhanced CT. *Acad Radiol* 2002;9(Suppl 1):S200–4. [PubMed: 12019869]
13. Weichert JP, Lee FT Jr, Chosy SG, Longino MA, Kuhlman JE, Heisey D, Levenson G. Combined hepatocyte-selective and blood pool contrast agents for CT detection of experimental liver tumors. *Radiology* 2000;216:865–71. [PubMed: 10966724]
14. Weichert JP, Longino MA, Bakan DA, Spigarelli MG, Chou T, Schwendner SW, Counsell RE. Polyiodinated triglyceride analogs as potential computed tomography imaging agents for the liver. *J Med Chem* 1995;38:636–46. [PubMed: 7861412]
15. Powers JF, Evinger MJ, Tsokas P, Bedri S, Alroy J, Shahsavari M, Tischler AS. Pheochromocytoma cell lines from heterozygous neurofibromatosis knockout mice. *Cell Tissue Res* 2000;302:309–20. [PubMed: 11151443]
16. Engler S, Thiel C, Forster K, David K, Bredehorst R, Juhl H. A novel metastatic animal model reflecting the clinical appearance of human neuroblastoma: growth arrest of orthotopic tumors by natural, cytotoxic human immunoglobulin M antibodies. *Cancer Res* 2001;61:2968–73. [PubMed: 11306475]
17. Weber SM, Peterson KA, Durkee B, Qi C, Longino M, Warner T, Lee FT Jr, Weichert JP. Imaging of murine liver tumor using microCT with a hepatocyte-selective contrast agent: accuracy is dependent on adequate contrast enhancement. *J Surg Res* 2004;119:41–5. [PubMed: 15126080]
18. Cleary S, Brouwers FM, Eisenhofer G, Pacak K, Christie DL, Lipski J, McNeil AR, Phillips JK. Expression of the noradrenaline transporter and phenylethanolamine N-methyltransferase in normal human adrenal gland and pheochromocytoma. *Cell Tissue Res* 2005;27:1–11.
19. Eisenhofer G, Walther MM, Huynh TT, Li ST, Bornstein SR, Vortmeyer A, Mannelli M, Goldstein DS, Linehan WM, Lenders JW, Pacak K. Pheochromocytomas in von Hippel-Lindau syndrome and multiple endocrine neoplasia type 2 display distinct biochemical and clinical phenotypes. *J Clin Endocrinol Metab* 2001;86:1999–2008. [PubMed: 11344198]
20. Yoshida-Hiroi M, Bradbury MJ, Eisenhofer G, Hiroi N, Vale WW, Novotny GE, Hartwig HG, Scherbaum WA, Bornstein SR. Chromaffin cell function and structure is impaired in corticotropin-releasing hormone receptor type 1-null mice. *Mol Psychiatry* 2002;7:967–74. [PubMed: 12399950]
21. Tischler AS, Powers JF, Alroy J. Animal models of pheochromocytoma. *Histol Histopathol* 2004;19:883–95. [PubMed: 15168351]
22. Michl P, Barth C, Buchholz M, Lerch MM, Rolke M, Holzmann KH, Menke A, Fensterer H, Giehl K, Lohr M, Leder G, Iwamura T, et al. Claudin-4 expression decreases invasiveness and metastatic potential of pancreatic cancer. *Cancer Res* 2003;63:6265–71. [PubMed: 14559813]
23. Garcia M, Fernandez-Garcia NI, Rivas V, Carretero M, Escamez MJ, Gonzalez-Martin A, Medrano EE, Volpert O, Jorcano JL, Jimenez B, Larcher F, Del Rio M. Inhibition of xenografted human melanoma growth and prevention of metastasis development by dual antiangiogenic/antitumor activities of pigment epithelium-derived factor. *Cancer Res* 2004;64:5632–42. [PubMed: 15313901]
24. Streck CJ, Zhang Y, Miyamoto R, Zhou J, Ng CY, Nathwani AC, Davidoff AM. Restriction of neuroblastoma angiogenesis and growth by interferon- $\alpha/\beta$ . *Surgery* 2004;136:183–9. [PubMed: 15300178]

25. Tischler AS, Shih TS, Williams BO, Jacks T. Characterization of pheochromocytomas in a mouse strain with a targeted disruptive mutation of the neurofibromatosis gene *Nf1*. *Endocr Pathol* 1995;6:323–35. [PubMed: 12114814]
26. Hill GD, Pace V, Persohn E, Bresser C, Haseman JK, Tischler AS, Nyska A. A comparative immunohistochemical study of spontaneous and chemically induced pheochromocytomas in B6C3F1 mice. *Endocr Pathol* 2003;14:81–91. [PubMed: 12746566]
27. Suri C, Fung BP, Tischler AS, Chikaraishi DM. Catecholaminergic cell lines from the brain and adrenal glands of tyrosine hydroxylase-SV40 T antigen transgenic mice. *J Neurosci* 1993;13:1280–91. [PubMed: 7680068]
28. Yu J, Pacak K. Management of malignant pheochromocytoma. *Endocrinologist* 2002;19:291–4.
29. Bravo EL, Tagle R. Pheochromocytoma: state-of-the-art and future prospects. *Endocr Rev* 2003;24:539–53. [PubMed: 12920154]
30. Eisenhofer G, Bornstein SR, Brouwers FM, Cheung NK, Dahia PL, de Krijger RR, Giordano TJ, Greene LA, Goldstein DS, Lehnert H, Manger WM, Maris JM, et al. Malignant pheochromocytoma: current status and initiatives for future progress. *Endocr Relat Cancer* 2004;11:423–36. [PubMed: 15369446]

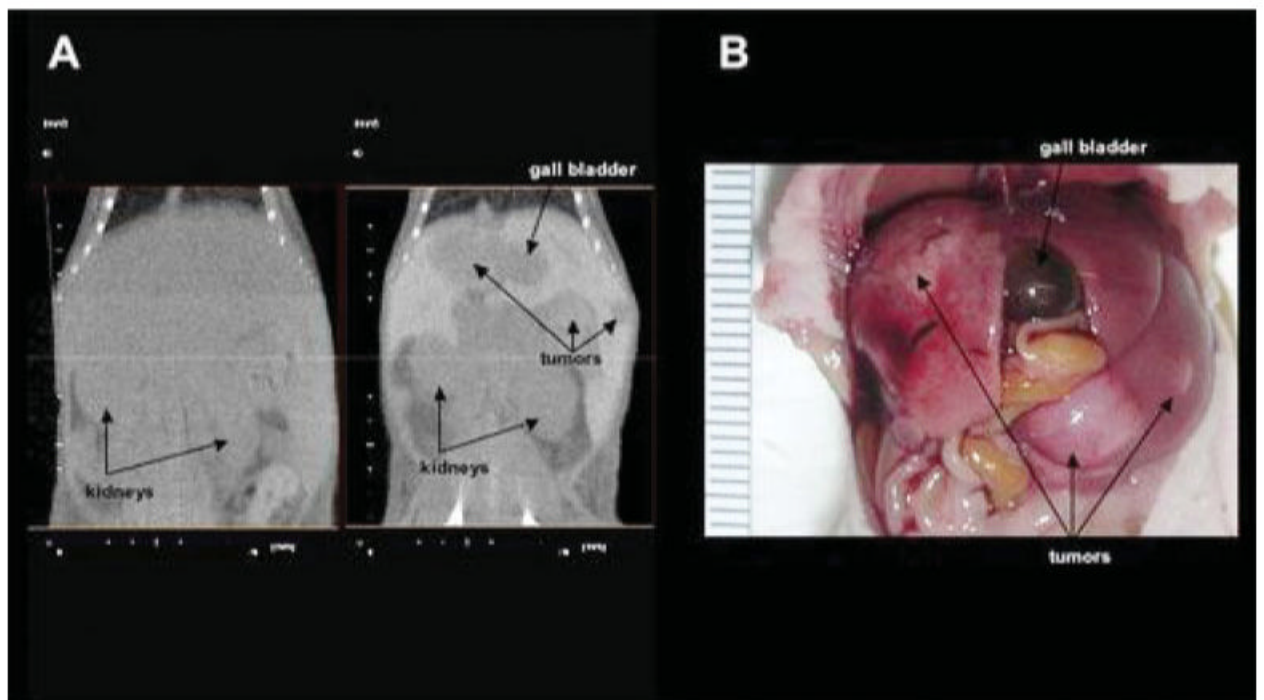




**FIGURE 1.** Serial DHOG hepatobiliary contrast-enhanced microCT scans reveal progression of MPC liver metastasis over time (arrows: tumors; Left: at 3 weeks, Middle: at 4 weeks, Right: at 5 weeks) Scale bar: 5.0 mm.

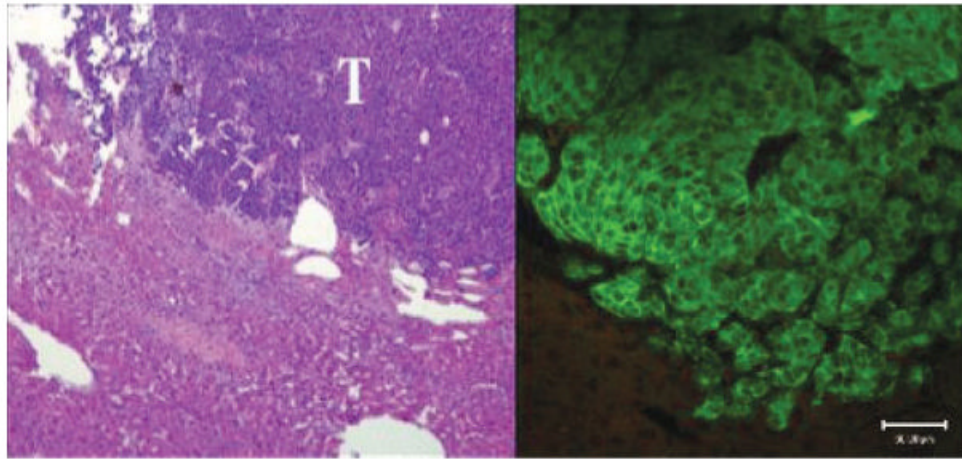


**FIGURE 2.** Three-dimensional image: High-resolution reconstruction of a microCT data set. Pixel for printing is  $842 \times 937 \text{ mm}^2$ .



**FIGURE 3.**

(a) MicroCT without and with DHOG contrast enhancement in the same mouse. Tumors are visualized only in the contrast-enhanced scan. (b) Macroscopic examination of the scanned mouse showing extensive liver metastases.

**FIGURE 4.**

Histopathology. Left: H&E stain. Tumors are composed of small basophilic cells (T, tumor) sharply delineated from the adjacent liver (magnification:  $\times 10$ ). Right: Immunohistochemical staining shows reactivity for tyrosine hydroxylase in the tumor. Similar staining is not present in hepatocytes (magnification:  $\times 25$ ). Scale bar: 50  $\mu\text{m}$ . Mean norepinephrine levels in liver metastatic lesions were 223,767 pg/mg. Mean epinephrine levels in liver metastatic lesions were 875 pg/mg.

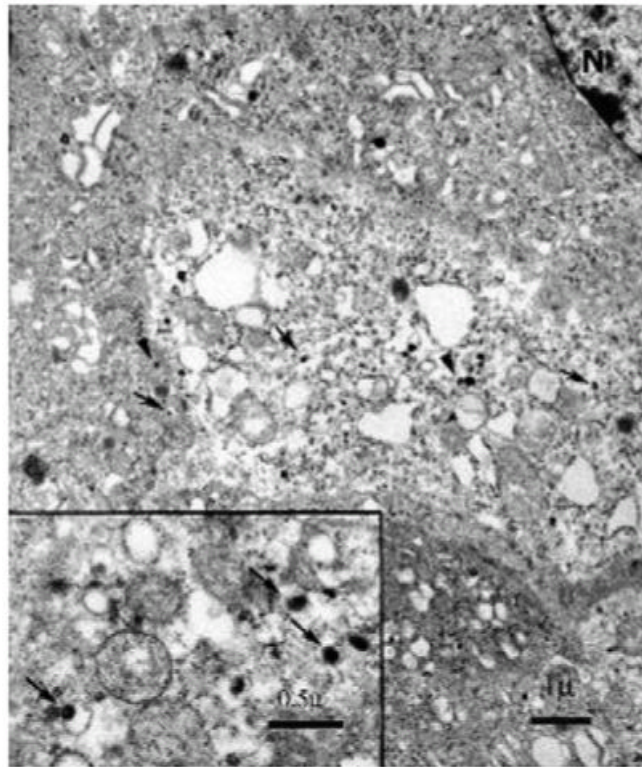


**FIGURE 5.** Characteristic membrane-bound secretory granules typically seen in pheochromocytoma with eccentric and centric dense cores and halos (arrows) visualized by electron microscopy (N, nucleus). Full-length arrows, norepinephrine producing granules (eccentric).<sup>20</sup> Arrow heads point epinephrine-producing granules (centric).<sup>20</sup> Scale bar: 1 or 0.5  $\mu\text{m}$ , respectively.